Stereo PIV investigation on fire ant alate wingbeat induced flow

Lichuan Gui, Dayong Sun, Tom Fink, Tim Menzel, John Seiner and Douglas Streett*

The National Center for Physical Acoustics, University of Mississippi
* USDA-ARS-BCMRRU, Stoneville

ABSTRACT

Tests were conducted to investigate the fire ant alate wingbeat induced flows with a stereo particle image velocimetry (SPIV) system. As shown in Figure 1, the test system includes a fog generator, a YAG laser, a set of light sheet optics, a test chamber, a three dimensional traverse, and two high-resolution digital video cameras. During the tests, a special fluid is injected into the heater of the fog generator by a syringe pump with a flow rate of 0.1 ml per minute to create fog particles of a few micro-meters in diameter. The fog is clean and not harmful for humans and the tested insects. Fresh air is mixed with the fog particles and driven by heat convection into the test chamber of 100×130×160 mm3 through a Ø75 mm aluminum pipe with a low flow speed that can be ignored in comparison to the fire ant wing beat induced flow velocity. The tested flying fire ant alate is tethered on a fine metal wire (Ø0.3mm) and held at the test position in the fog chamber by the 3-D traverse system. A pulsed beam from a Nd:YAG laser is converted to a thin (≈0.5 mm) light sheet in the test region through a set of light sheet optics that includes a cylindrical divergent lens, a mirror and a cylindrical condenser lens. The laser is controlled by a delay & pulse generator (not shown in Fig.1) so that double laser pulses of 50 μs time interval are sent out at repeating rate of up to 30 Hz to illuminate the fog particles in the light sheet. Two PCO 2000 cameras, i.e. camera A and B, are synchronized to the laser pulses with the delay & pulse generator to acquire particle image recording pairs. Camera A views the test plane with a normal configuration so that there is no image deformation in the PIV recordings. The lens axis of camera B is rotated from the normal direction by 45°, so that the velocity component perpendicular to the test plane can be measured. To focus precisely with the rotated lens, the image sensor of camera B is rotated with a proper angle to fulfill the Scheimpflug condition. Since the PIV recordings acquired with camera B have strong image distortion, an image calibration method is adopted to correct the distorted images.

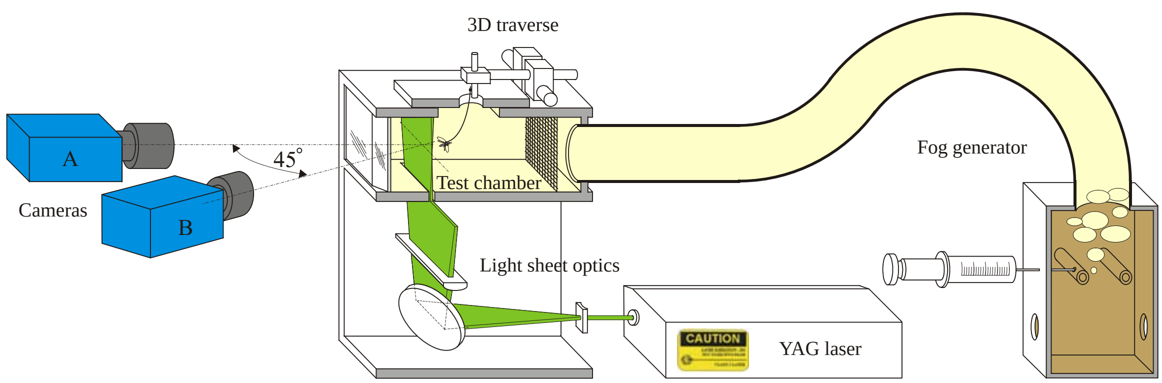

Figure 1: Experimental setup for SPIV tests on fire ant alate wingbeat induced flows

Tests were conducted with two configurations, i.e. (1) sideview test that measures air flow velocity distribution in a vertical plane that goes through the fire ant body axis, and (2) rearview test that is for the velocity distribution in a vertical plane that is perpendicular to the first plane and about 2 mm behind the fire ant alate body. In the sideview test, part of the light sheet was blocked so that the laser did not directly hit the fire ant, and the fire ant body and wings were illuminated with scattered laser light and clearly imaged in the PIV recordings. The fire ant wing images were used to determine the phase. In the rearview test, the fire ant alate was 2 mm off the light sheet and illuminated with the scattered light, so that it was imaged in the background of the PIV recording. A low-pass digital filter was used to enhance the dark images of fire ant wings to determine the phase, and a high-pass filter was used to remove the fire ant alate image to reduce the noise for determining the air flow velocity. The PIV recordings were evaluated with a correlation-based algorithm to determine instantaneous velocity vector maps. Over 10,000 velocity vector maps were obtained for each test case and divided in to about 20 phase groups. A statistical analysis was conducted for each phase with more than 400 velocity maps.

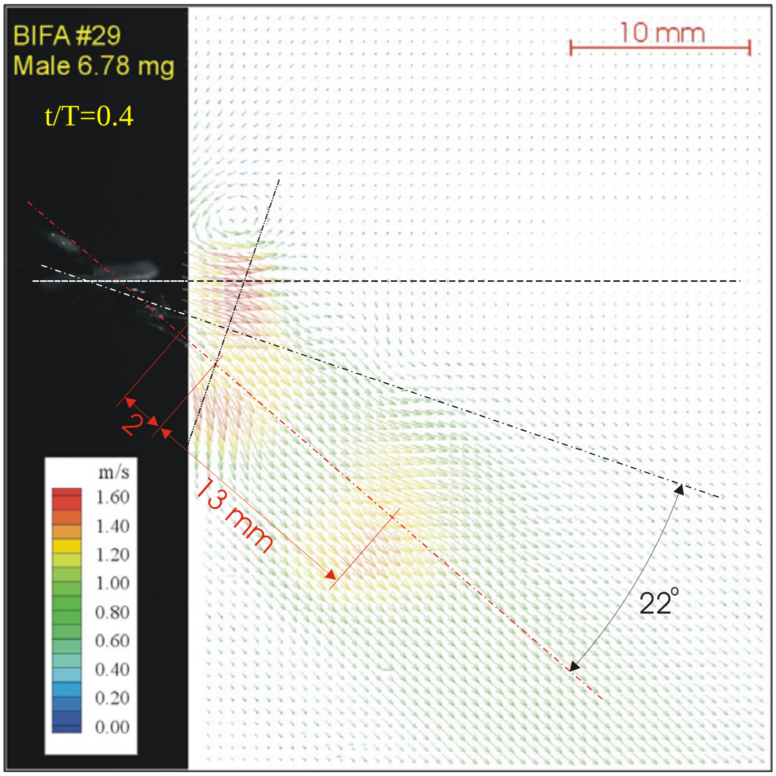

Figure 2: Sideview velocity distribution at t/T=0.4

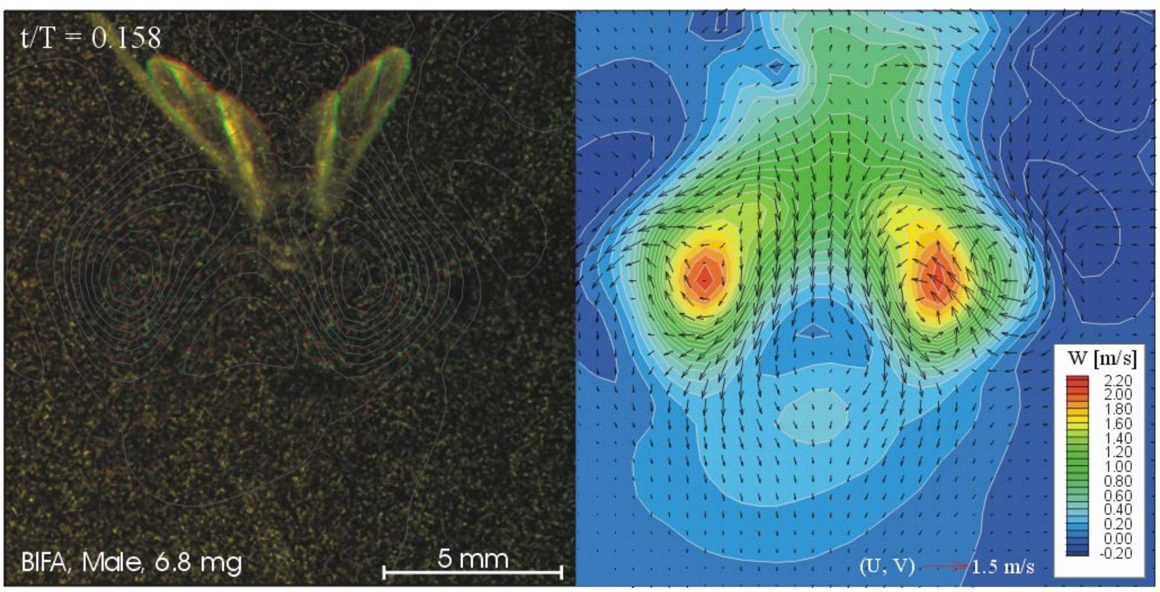

Figure 3: Rearview velocity distribution at t/T=0.158

Test results are shown in this poster for a black imported male fire ant alate weighting 6.78 mg. It was a strong flyer with wing beat frequency of around 120 Hz. Photos of the tested fire ant body and wings are shown in Fig. 3 on the top left and right corners. Fig. 2 shows the mean velocity vector map for the sideview test at relative phase t/T=0.4. In this case, there is a 19° tethering angle between the fire ant body axis and the horizontal direction. The main flow direction deviates from the ant body axis by 22°. Only two velocity components are obtained in the sideview test because the third component can be ignored in the central vertical plane. The vector map demonstrates a pulsed flow. The high-speed center of the pulsed flow moves 13 mm downstream in the wingbeat period with speed of 1.6 m/s that equals the maximal velocity in the central vertical plane. The development of the pulsed flow can be seen in Fig. 3, and it is shown that the high-speed center appears in the beginning of the wingbeat period (that is defined when the forewing tip reaches the highest position); then it develops to a maximal size of 9x11 mm2 at t/T=0.7; and finally it disappears in the next wingbeat period at t/T=0.63 when the forewing tip begins to move upwards. A vortex street can be seen aside the pulsed flow path. The location of the rear view test plane is indicated in Fig. 2 with a dash-double-dot line, i.e. 2 mm downstream from the rear part of the fire ant alate. One of the rear view test results are given in Fig. 3. The vectors represent the velocity components in the test plane, whereas the contours represent the distribution of the perpendicular velocity component that is directed downstream. Note that in the rearview test case the fire ant body axis was adjusted so that it is almost in the horizontal plane. Test results for 19 different phases show that the downstream velocity distribution in the test plane have two high-speed centers that are generated at t/T=0.84 in the previous period and approach the maximal value of around 2.0 m/s at t/T=0.16, and merge together at t/T=0.63. Assume that the high-speed center of the downstream velocity starts in the wingbeat stroke plane and moves about 8 mm downstream to the test plane with speed of 2.0 m/s, it takes 4 ms, i.e. 48% of the 8.3-ms wingbeat period. Since the maximal downstream velocity moves to the test plane at t/T=0.16, it should be in the wingbeat stroke plane at t/T=0.68 of in the previous period. It can be concluded that the propulsion of the flight is generated when the wings move back in the late portion of the wingbeat period. More detailed analysis will be further completed and reported later.

(Current research was supported by USDA 58-6402-6 NCPA to Dr. Henry Bass.)